

Silicon based organic semiconductor laser

A. E. Vasdekis, S. A. Moore, A. Ruseckas, T. F. Krauss, I. D. W. Samuel,^{a,b)} and G. A. Turnbull^{a,c)}

Organic Semiconductor Centre and Ultrafast Photonics Collaboration, SUPA, School of Physics and Astronomy, University of St. Andrews, St. Andrews, Fife KY16 9SS, United Kingdom

(Received 20 May 2007; accepted 2 July 2007; published online 2 August 2007)

The authors demonstrate silicon based visible lasers as potential optical interconnects by combining silicon processed resonators and solution processed light-emitting polymers. The high refractive index and absorption coefficient of silicon at these wavelengths were addressed by developing distributed Bragg reflector resonators on a silicon-on-insulator substrate. The performance of the hybrid structure was characterized and analyzed in comparison to an all-silica counterpart and mechanisms for controlling the number of longitudinal modes and for tuning the emission wavelength were explored. © 2007 American Institute of Physics. [DOI: 10.1063/1.2764553]

Silicon based photonic devices have received significant attention in recent years due to their potential for cost-effective integrated components for optical communications and interconnects.^{1,2} A major hindrance toward this aim is the poor optical emission efficiency of silicon. To overcome this, several approaches have been proposed, including optically excited Raman³ and nanopatterned silicon⁴ lasers, quantum confinement in silicon nanocrystals,^{5,6} the use of rare earth dopants,⁷ and the bonding of III-V semiconductor lasers to silicon chips.⁸ In this letter, we propose an alternative approach that combines microstructured silicon resonators with light-emitting organic semiconductors. Despite the substantial absorption of silicon in the visible, under optical excitation the hybrid silicon-polymer structure operates as a red surface-emitting laser. Integration of the solution-processable polymer adds only a simple supplementary fabrication step, compatible with standard complementary metal-oxide-semiconductor processing. The emission wavelength of the polymer lies within the absorption band of silicon photodetectors, and so could provide a cost-effective route to chip-to-chip optical interconnects.²

Microstructured organic semiconductor lasers have attracted growing interest in recent years⁹ and their simple solution deposition makes them good candidates for adding coherent light emission to silicon. However, their integration on silicon introduces two significant challenges: the substantial absorption of silicon at the wavelengths of the polymer photoluminescence and the high refractive index of silicon, which presents complications for confining the laser emission within a polymer waveguide. We address these through a distributed Bragg reflector (DBR) resonator design, based on a silicon-on-insulator (SOI) substrate. Two periodically microstructured silicon segments act as mirrors, while the silicon epilayer between these is removed, exposing the buried SiO₂ layer. A thin film of the organic amplifying medium covers the whole structure (Fig. 1). Due to the boundary conditions at the air-polymer and polymer-SiO₂ interfaces, a polymer waveguide is formed between the two silicon mirrors with a confinement factor limited only by the thickness of the polymer layer. The area between the two periodically

microstructured silicon reflectors acts as a long “defect,” breaking the symmetry of the periodic silicon photonic lattice. The introduction of the polymer defect also served as a method to minimize the interaction of the laser light with the silicon regions and address the high absorption coefficient of silicon.

The SOI substrates (Soitec) had a 220 nm thick undoped silicon epilayer on top of a 2 μm thick silicon dioxide layer on a silicon substrate. The thickness of the epilayer was initially decreased from 220 to 30 nm using reactive ion etching (RIE), based on a gas mixture of CHF₃ and SF₆ at a ratio of 1:1. The Bragg mirrors were defined using electron beam lithography [LEO Gemini 1530 scanning electron microscopy (SEM)/RAITH ELPHY lithography system] on polymethylmethacrylate. A lift-off step was performed after the evaporation of 30 nm of Ni that acted as an etch mask. The pattern was transferred to the silicon epilayer using RIE based on the same gas mixture as for the initial thinning process.

The silicon microstructured mirrors were made of linear gratings with a period of 360 nm and a fill factor of 30%. For this lattice constant and at the wavelength of 630 nm, the stop band of these Bragg mirrors originates from second order diffraction and provides both feedback and coupling of the laser mode to free space radiation.¹⁰ The mirrors were spaced by 50 μm and the whole structure was coated from

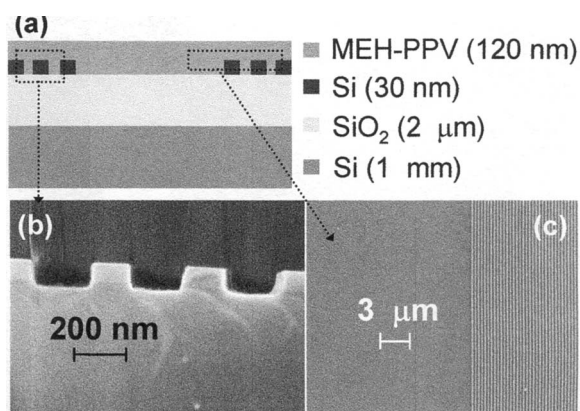


FIG. 1. (a) Schematic of the Si-polymer hybrid laser. (b) SEM image of the side of the silicon grating mirror. (c) SEM image of a top view detail of the mirror and the defect area.

^{a)} Author to whom correspondence should be addressed.

^{b)} Electronic mail: idws@st-andrews.ac.uk

^{c)} Electronic mail: gat@st-andrews.ac.uk

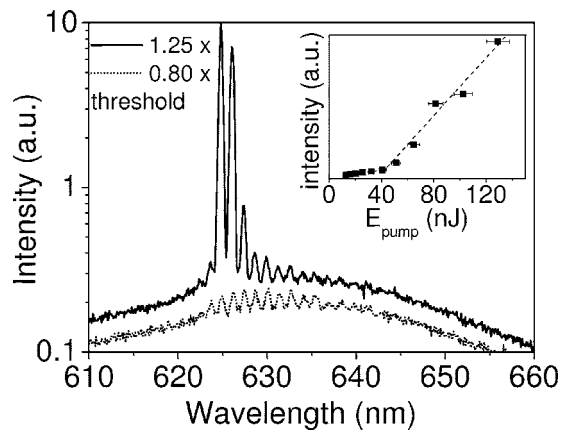


FIG. 2. Emission spectra above and below threshold for a silicon based cavity with a $50\ \mu\text{m}$ mirror separation. Inset: the input-output relationship.

chlorobenzene solution with a 120 nm thick film of the prototypical conjugated polymer poly[2-methoxy-5-(2'-ethyl-hexyloxy)-*p*-phenylene vinylene] (MEH-PPV).¹¹ At this thickness, only the fundamental transverse electric mode is supported in the spectral region of the polymer gain.

The laser characterization involved the optical excitation of the hybrid structures using 1.2 ns pulses at 532 nm from a frequency-doubled microchip laser. The pump beam was focused to an excitation area of $85\ \mu\text{m}$ in diameter, centered in the area between the mirrors. The emission from the polymer laser was collected from the surface using a fiber-coupled charge-coupled device (CCD) spectrometer of $2\ \text{\AA}$ resolution. To avoid photo-oxidation, the polymer films were held under vacuum of 10^{-4} mbar during operation.

The emission spectra below and above the lasing threshold for a cavity with a $50\ \mu\text{m}$ mirror separation are shown in Fig. 2. Below threshold, the spontaneous emission from the conjugated polymer couples to optical modes with frequencies within the stop band of the Bragg mirrors and intensity primarily localized in the defect area.¹⁰ These modes manifest themselves in a series of narrow peaks, spaced at $\Delta\lambda = 1.25\ \text{nm}$. For excitation energies above 45 nJ, the intensity of the lower wavelength resonant modes increases at a faster rate indicating the laser threshold (inset of Fig. 2) and at higher pumping levels they dominate the emission spectrum. Not all of the longitudinal modes reach threshold and this is attributed to the different scattering and absorption mirror losses that each mode experiences.

In order to further investigate the performance of the hybrid polymer-silicon lasers, we compared their lasing characteristics with those of DBR cavities of similar dimensions, but fabricated on fused silica substrates. The mirrors in this case were fused silica gratings with a period and depth of 410 and 80 nm, respectively, while the mirror separation was $50\ \mu\text{m}$. The structured substrate was coated with a 120 nm thick MEH-PPV film as before to complete the laser. In this structure, in addition to the defect modes, we observe two additional broad peaks below threshold at wavelengths of 627 and 636 nm (denoted by the arrows in Fig. 3). These peaks were found to separate in wavelength as the observation angle moves away from the normal to the substrate, in contrast to the defect modes, which show no dispersion. We identify these modes as band-edge Bloch modes, localized in the periodic lattice.¹⁰ We attribute their absence in the silicon

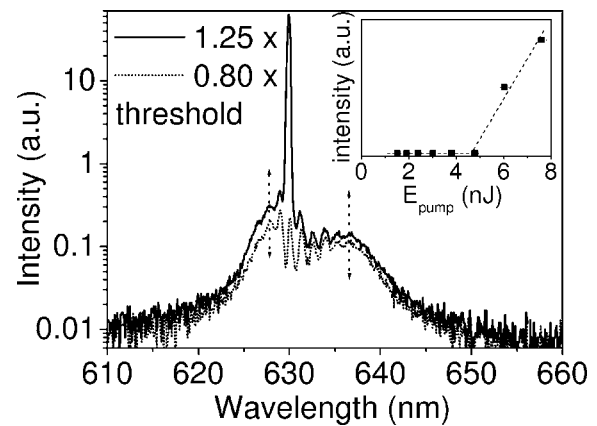


FIG. 3. Emission spectra above and below threshold for a SiO_2 based cavity with a $50\ \mu\text{m}$ mirror separation. Inset: the input-output relationship.

case to the high absorption coefficient of silicon at these wavelengths.

Above a pumping threshold of 4.7 nJ, we observe single frequency lasing at 630 nm (inset of Fig. 3). The reduced threshold of the all-silica resonator is also indicative of the lower absorption losses in these mirrors at the lasing wavelengths. This was quantified through a comparison of the threshold gains in the silicon and SiO_2 based lasers, which are equal to the sum of the polymer waveguide and mirror losses. The waveguide loss for MEH-PPV films is approximately¹² $20\ \text{cm}^{-1}$ and the gain at threshold was determined via the product of the stimulated emission cross section for MEH-PPV and the singlet exciton density. The exciton density was calculated by numerically solving the exciton rate equation [Eq. (3) in Ref. 11], where the exciton lifetime and exciton-exciton annihilation were taken into account and the temporal profile of the pump pulse was assumed to have a top hat shape. We found that the gains at threshold for the SiO_2 and silicon mirrors based lasers were 294 and $371\ \text{cm}^{-1}$, respectively, indicating that the modal reflectivities are 26% and 17% in each case. The in-plane reflectivities are both quite low due to the surface emission losses from the Bragg mirrors. The difference between them is attributed to the absorption losses of the silicon and is the origin of the observed threshold energy difference. The single frequency operation in the SiO_2 case suggests the presence of wavelength dependent out-of-plane radiation losses across the mirror stop band.¹³ These are absent in the silicon based laser, possibly due to the dominant absorption losses.

Achieving lasing in cavities only $50\ \mu\text{m}$ long shows the high gain of conjugated polymers, though it does lead to higher threshold densities ($600\ \text{kW}/\text{cm}^2$ for the silicon $65\ \text{kW}/\text{cm}^2$ for the silica resonators) than in some other polymer laser work. In comparison, in 1 mm long MEH-PPV waveguides amplified spontaneous effect can be observed at density of $10\ \text{kW}/\text{cm}^2$,¹⁴ while in other organic semiconductors, lasing thresholds can be less than $100\ \text{W}/\text{cm}^2$ in a 9 mm long device.¹⁵ However, the short resonators allow for very compact lasers operating with low optical pumping energies.¹⁰ The resulting polymer optical gains are similar to that observed in both silicon nanocrystals ($\sim 100\ \text{cm}^{-1}$) (Ref. 5) and nanopatterned crystalline silicon ($\sim 260\ \text{cm}^{-1}$, albeit at a temperature of 10 K),⁴ and larger than typically observed in Si Raman lasers.

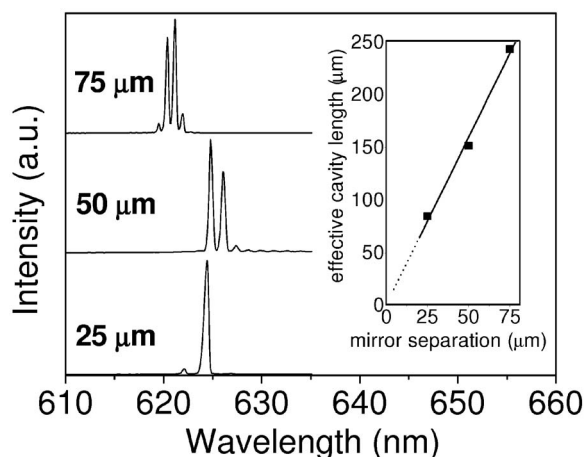


FIG. 4. Broadening of the laser spectra for increasing cavity length. Inset: the relationship between the physical length of the mirror separation and the effective cavity length.

In the silicon resonators, the number of resonant modes may be controlled by the length of the mirror separation. In Fig. 4, the surface-coupled emission spectra for three different cavity lengths are plotted at an excitation level of 1.25 times above threshold. An increase in the mirror separation, and hence of the effective cavity length, causes the laser spectrum to broaden and comprise more closely spaced longitudinal modes. The effective cavity length was deduced from the mode spacing and its relationship with the length of the mirror separation was found to be linear with a slope of 3.1 (inset of Fig. 4). This value corresponds to the group index of the polymer waveguide¹⁶ and is in reasonable agreement, within experimental error, with the calculated value of 2.7, where both the waveguide and material dispersion were taken into account.¹⁷ The simultaneous presence of multiple longitudinal modes is favored by the broadband gain spectra of conjugated polymers,¹¹ a potential advantage for communication applications due to the possibility of parallel information processing.¹⁸ This potential was further explored by investigating ways of tuning the wavelength of the hybrid Si-polymer lasers. By changing the lattice constant from 360 to 330 nm, the laser emission could be blueshifted by almost 20 nm. The wavelength is also strongly dependent on the silicon grating thickness. For example, when the epilayer thickness was increased to 220 nm, a reduction in grating period of 80 nm was required to maintain lasing at 630 nm. The relationship between grating period and lasing wavelength in both cases were found to be in good agreement with transfer matrix calculations.¹⁹

In conclusion, we have demonstrated that conjugated polymers provide a convenient and simple way of adding light emission to silicon. In addition, we have demonstrated gain and lasing at room temperature in spite of using strongly absorbing silicon to form the resonator. The laser

emission wavelength may be tuned through the broad gain spectrum of organic semiconductors without the need for modulating the excitation wavelength. The light emission is in the visible region of the spectrum, so it is readily detected by silicon photodiodes, making it suitable for low cost chip-to-chip communications. Our laser is surface emitting, which is also convenient for this purpose. At present the laser is optically pumped, but we can envisage using the underlying silicon chip to apply a field or inject charge to modulate the light emission. In the longer term, electrically pumped lasing using *p*-doped silicon as a hole injection layer²⁰ is also a possibility.

The authors are grateful to EPSRC for financial support and to Covion (now Merck OLED Materials GmbH) for the supply of MEH-PPV. One of the authors (A.E.V.) gratefully acknowledges the Wingate Foundation for the fellowship support for this work. One of the authors (G.A.T.) holds an EPSRC Advanced Research Fellowship and another author (I.D.W.S.) holds an EPSRC Senior Research Fellowship.

- ¹G. T. Reed and A. P. Knights, *Silicon Photonics: An Introduction* (Wiley, Chichester, West Sussex, 2004), p. 57.
- ²D. A. B. Miller, *IEEE J. Sel. Top. Quantum Electron.* **6**, 1312 (2000).
- ³H. Rong, R. Jones, A. Liu, O. Cohen, D. Hak, A. Fang, and M. Paniccia, *Nature (London)* **433**, 725 (2005).
- ⁴S. G. Cloutier, P. A. Kosyrev, and J. Xu, *Nat. Mater.* **4**, 887 (2005).
- ⁵L. Pavesi, L. Dal Negro, G. Mazzoleni, G. Franzo, and F. Priolo, *Nature (London)* **408**, 440 (2000).
- ⁶M. Makarova, J. Vuckovic, H. Sanda, and Y. Nishi, *Appl. Phys. Lett.* **89**, 221101 (2006).
- ⁷H. Enner, G. Pomrenke, A. Axmann, K. Eisele, W. Haydl, and J. Schneider, *Appl. Phys. Lett.* **46**, 381 (1985).
- ⁸A. W. Fang, H. Park, O. Cohen, R. Jones, M. J. Paniccia, and J. E. Bowers, *Opt. Express* **14**, 9203 (2006).
- ⁹I. D. W. Samuel and G. A. Turnbull, *Chem. Rev. (Washington, D.C.)* **107**, 1272 (2007).
- ¹⁰A. E. Vasdekis, G. Tsiminis, J.-C. Ribierre, L. O. Faolain, T. F. Krauss, G. A. Turnbull, and I. D. W. Samuel, *Opt. Express* **14**, 9211 (2006).
- ¹¹D. Amarasinghe, A. Ruseckas, A. E. Vasdekis, M. Goossens, G. A. Turnbull, and I. D. W. Samuel, *Appl. Phys. Lett.* **89**, 201119 (2006).
- ¹²M. Goossens, A. Ruseckas, G. A. Turnbull, and I. D. W. Samuel, *Appl. Phys. Lett.* **85**, 31 (2004).
- ¹³A. Hardy, D. F. Welch, and W. Streifer, *IEEE J. Quantum Electron.* **25**, 2096 (1989).
- ¹⁴F. Hide, M. A. DiazGarcia, B. J. Schwartz, M. R. Andersson, Q. B. Pei, and A. J. Heeger, *Science* **273**, 1833 (1996).
- ¹⁵A. Rose, Z. Zhu, C. F. Madigan, T. M. Swager, and V. Bulovic, *Nature (London)* **434**, 876 (2005).
- ¹⁶Y. O. Barmenkov, D. Zalvidea, S. Torres-Peiró, J. L. Cruz, and M. V. Andrés, *Opt. Express* **14**, 6394 (2006).
- ¹⁷A. E. Vasdekis, G. A. Turnbull, I. D. W. Samuel, P. Andrew, and W. L. Barnes, *Appl. Phys. Lett.* **86**, 161102 (2005).
- ¹⁸M. A. Foster, A. C. Turner, J. E. Sharping, B. S. Schmidt, M. Lipson, and A. L. Gaeta, *Nature (London)* **441**, 960 (2006).
- ¹⁹A. Yariv and P. Yeh, *Optical Waves in Crystals* (Wiley, New York, 2003), p. 155.
- ²⁰G. G. Qin, A. G. Xu, G. L. Ma, G. Z. Ran, Y. P. Qiao, B. R. Zhang, W. X. Chen, and S. K. Wu, *Appl. Phys. Lett.* **85**, 5406 (2004).